Development and Basic Calibration of an Acoustic Vector Network Analyser

Marcus MacDonell
Department of Engineering
University of Waikato
Hamilton, NZ

Jonathan Scott
Department of Engineering
University of Waikato
Hamilton, NZ

***Abstract*—This project aims to develop a method that drastically improves measurement of the acoustic properties of objects. Previous research at the University of Waikato has made progress with acoustic technologies as a precursor to a dual port vector network analyser. These technologies have been furthered to this end by 3D printing a modified coupler that now includes a flange with alignment pins, and a groove to house an O-ring as well as a number of other "custom" components for the coupler assembly. This assembly has been interfaced successfully with a VNA and collected data, this process is not straightforward and requires carefully thought-out adjustment to produce sensible data. Complicating this process is the vast difference in propagation speeds for acoustic and electromagnetic signals. The swept measurements performed show promising results that further prove the hardware and indicate that particular calibration terms namely those for isolation that are normally ignored in the electromagnetic domain are potentially crucial in the acoustic domain.**

***Index Terms*—Vector Network Analysis, Waveguide, Acoustic.**

I. Introduction

This project aims to develop a method that drastically improves measurement of the acoustic properties of objects. These objects can be measured using manual techniques, but these techniques are often impractical or too uncertain [1]. We aim to achieve fast, easy, traceable measurements by applying the lessons from six decades of highly successful research into fast, traceable microwave electromagnetic (EM) network measurements to the acoustic domain to develop an Acoustic Vector-corrected Network Analyser (AVNA). The instrument will take the form of a test set that integrates with a commercial electromagnetic Vector-corrected Network Analyser, and a set of carefully modeled standards. A key step in the development of this measurement system is the construction of an acoustic test set, remote heads and calibration standards, this paper discusses the development of these crucial elements.

This concatenation of techniques is possible because the wavelengths of sound waves in air and water are comparable to the wavelengths of radio waves in free space. There are many modern applications of acoustic measurement. These include, but are not limited to the following: Characterising the absorption of sound by furnishings or architectural materials, estimating dry matter yield of pasture via its acoustic permeability, tuning the impedance presented by wind or brass instruments, establishing the safety margin of ear plugs by traceable measurement of their transmission of sound as a function of frequency, finding the frequency response of various ear canal shapes, measuring the sonar cross section of an insect you wish to detect or the reflection from a torpedo that you might wish to conceal, the reflectivity of a tumour you seek with ultrasound, optimising energy loss in a muffler, or the undesirable transmission of sound through an air duct. All of these measurement challenges are approached crudely, looking as did their electromagnetic equivalents in the 1950s and early 1960s.

Technical advances in electromagnetic measurement spanning the last 60 years have led to the VNA that can be purchased today [2]. VNAs are manufactured by a number of global companies, for example Keysight Technologies in the USA, Rhode & Schwarz in Germany, Anritsu based out of Japan, and Copper Mountain sourced from Russia. Although the VNA is accepted as the most precise and versatile measurement instrument available to radio-frequency and microwave designers, clever advances continue to appear, especially in the arena of calibration and traceability. These improvements are spurred on by the advance to millimeter-wave and terahertz domains.

Low-cost, single-box commercial VNAs are available with operating bandwidths from low frequency up to 500 MHz; more expensive units reach 67 GHz. This implies free space wavelengths from many meters down to 600 mm in the case of the low-cost units, or down to about 5 mm for the 67 GHz flagship machines. When higher frequencies are required, or waveguide ports are needed, it is customary for the instrument to be extended from the single box by means of remote measurement heads, providing an outboard test set. Provision is made on many VNAs for the attachment of such remote heads. These may be manufactured in house, or supplied to the manufacturer by a third party. In the case of Keysight Technologies, suppliers such as OML Microwave or Virginia

The Authors would like to thank SFTI for funding this research.

Diodes provide the remote head components.

Acoustic measurement of network properties for sound and vibration application, in contrast, is an underdeveloped but very important technology. Equipment supplied by the likes of Brüel & Kjær, a leader in the field, is not vector corrected, and is rarely traceable to national standards. Measurements are often laborious, mechanical, and expensive. An Acoustic VNA provides a solution to these problems.

Two standards outline current methods for measuring acoustic impedance: ISO 10534-1:1996 and ISO 10534-2:1998. These standards rely on 'Impedance tubes' and use the 'standing wave ratio' or 'transfer function' methods respectively [10] [11]. The AVNA addresses the issues of applying laborious methods by being able to perform swept measurements of the parameter of interest directly. To do this the AVNA will require some known standards. Although these standards do not yet exist, it is expected that they will be analogous to those required for a TRL or TRM calibration.

Acoustic impedance is the effective resistance of a material to vibration. In the case of solids impedance is therefore related to many familiar material properties like stiffness (Young's modulus) and hardness but also it's geometry and structure. These properties in combination contribute to the amount of energy transmitted through the material via vibration and the amount of energy reflected from the interface. S-parameters of a VNA describe the transfer of energy in terms of source and sink. In a dual port system the subscripts of the S-parameter describe the port the energy originated from and the port the energy was received. For example energy transmitted is S_{21} and energy reflected is S_{11}.

The following sections detail the development of the hardware for the AVNA as well as indicative measurements of materials whose acoustic properties are somewhat known such as stiff metals, foam and earplugs to show that the hardware is functional.

II. Hardware

Previous work at the University of Waikato has made progress with acoustic waveguide showing that 3D printing enables effective scaling to mm waveguide [3] and that a sliding load enables the approximation of an ideal acoustic load [4]. This body of research led to the desire to calibrate a reflectometer, i.e a single port measuring S_{11} [4]. Calibrating a single port is difficult to do because there does not exist an analogous acoustic standard for the 'open' in the standard '12 term' calibration process. The inability of most existing VNAs of appropriate bandwidth to perform calibrations intended for waveguide (8 term model etc) further complicates the problem. Following a single port calibration the logical next step is the calibration of a dual port system. The dual port system is envisaged to look much like a modern VNA system with remote heads. An example of such a system is shown in figure 1.

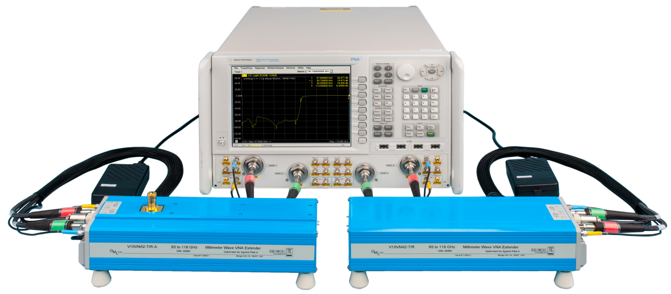

Fig. 1. A Keysight Performance Network Analyser system with remote heads containing all the mm-Wave components. [12]–[14]

The indicative measurements presented in this manuscript aim to verify the operation of acoustic remote heads constructed in-house, and to be used in conjunction with an early generation HP/Agilent 4395A vector network analyser. We essentially show uncalibrated Smith charts that indicate the system as a whole is functioning as expected, i.e., demonstrating directional separation.

A. Flange Design

This project continues work done with the acoustic directional coupler design of Lagasse [5]. The design, scaled to work in the upper half of the audible spectrum (10–20 kHz), is realised using 3D printing. A second set of heads, scaled for 1–2 kHz, is being constructed using conventional workshop facilities out of transparent acrylic.[1]

A major historical issue in the advance of microwave components was the development of a satisfactory standard for connecting waveguides, i.e., the flange design. We have, likewise, had to design a mechanical arrangement for connection of components. The larger heads destined for use from 1–2 kHz are less demanding, just as high-power waveguide for L-band (frequency 1–2 GHz, wavelength 150–300 mm) is straightforward. Nevertheless, mechanical stresses have demanded that the flanges in this system be made stronger. The directional coupler from [3] has been modified to include a flange with alignment pins, and a groove to house an O-ring. This is required to obtain good alignment and an air-tight seal. An example of the new flange design can be seen in figure 2. This figure presents the design of a short through length that is intended to be used in the 2-port calibration procedure.[2]

[1]The use of two coupler sets, and the chosen frequency ranges, exercises the two fabrication technologies. The physically larger set, and the use of transparent acrylic, makes for a system whose inner form is plainly visible and easier to explain.

[2]Although beyond the scope of this manuscript, we feel the need to point out that one of the challenges in the design is determining the "electrical length" of a piece of guide in the acoustic world. In the case of EM radiation, air is virtually indistinguishable from space, but in the acoustic world the air is the medium of energy transfer, and temperature, humidity, and the like affect the speed of propagation.

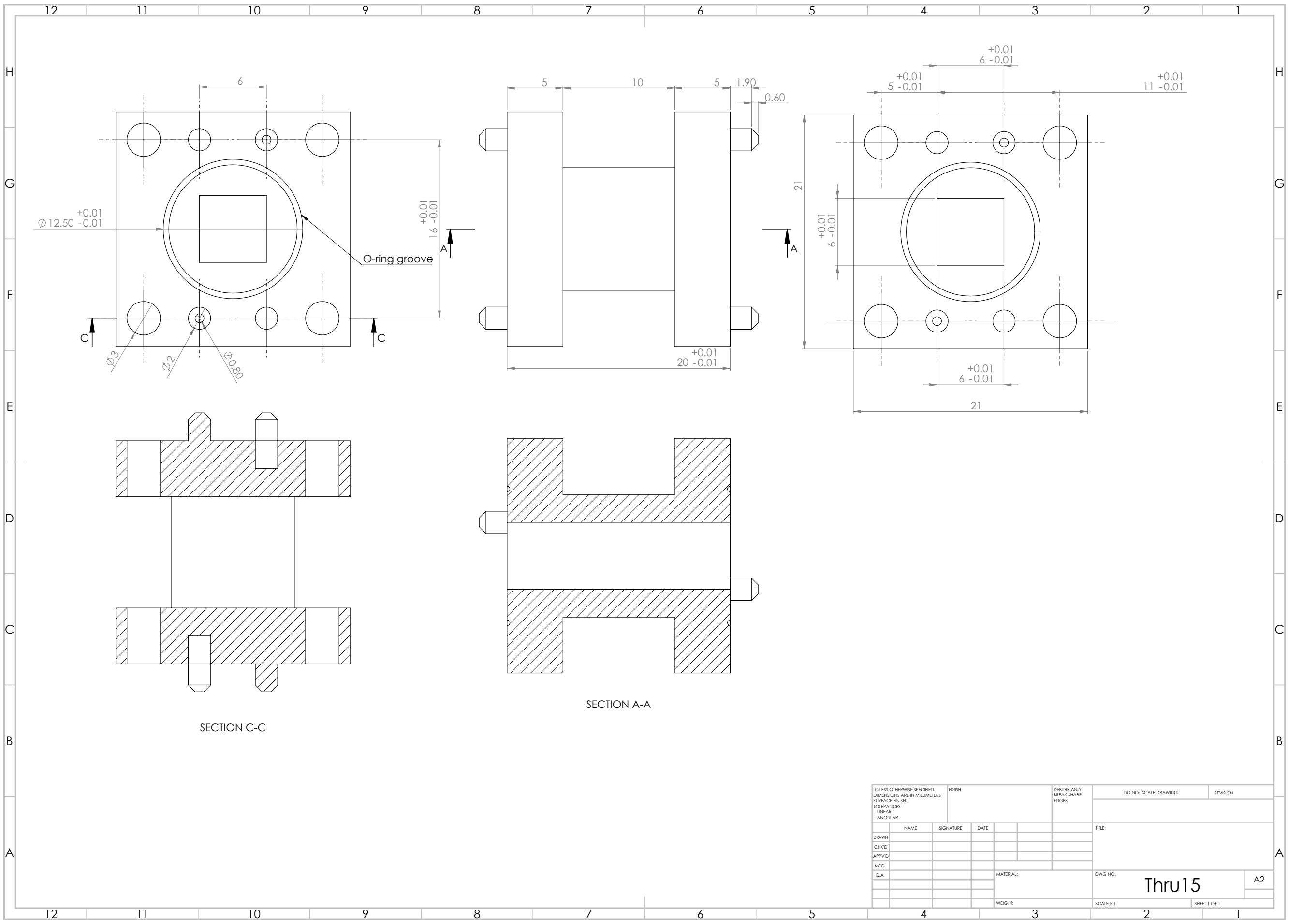

Fig. 2. Solidworks technical drawing of a proposed Thru to be 3D printed for calibrating the dual port system.

A number of other "custom" components are needed. For example, a waveguide horn for the attachment of the driver and mounting holes for MEMS microphones. These are the acoustic equivalent of the electromagnetic structures that introduce waves to the guide or collect and rectify waves in detectors, etc.

It will only be after calibration that the repeatability of guide junctions can be assessed. Nevertheless, we have some confidence. This kind of "bootstrapping" occurred a lot in the early development of microwave systems, which explains why it took 50 years to get from a few GHz to a few hundred GHz. We hope to short-circuit much of this in the acoustic domain by learning from the EM mm-Wave domain.

B. VNA Interface

A block diagram of the required hardware for an AVNA is shown in Figure 3. A large portion of the required hardware can be found in the 4395A, but the rest must be custom built to interface with the 4395A. An 87511A test-set has been retro-fitted with the remaining hardware and capacity to connect the acoustic waveguide heads.

Figure 4 is a block diagram of the Agilent 87511A test-set as configured to measure the reflection coefficient S_{11}. This block diagram shows the switching and coupler layout of the test-set in the electromagnetic domain that must be replicated in the acoustic domain.

It should be noted that the 4395A does not support TRL (Thru, Reflect, Line) or TRM (Thru, Reflect, Match) calibration methods, nor any waveguide calibration standards. [7] This is because, with a maximum operating frequency of 500 MHz, the designers did not imagine it would ever have waveguide application, or be used in situations where SOLT (Short, Open, Load, Thru) calibration might not be able to achieve more than enough accuracy. All of these will be implemented in a controlling computer, treating the VNA as a simple synthesiser with three channels of phase-resolving receivers.

The test setup to measure S_{11} has been realised with the hardware seen in Figures 5 & 6. The hardware is comprised of a block of amplifiers, loudspeaker, microphones and cabling. The amplifiers on the PCB are to drive the loudspeaker and to amplify the microphone signals specifically to interface with the 50 Ω input ports on the HP4395A.

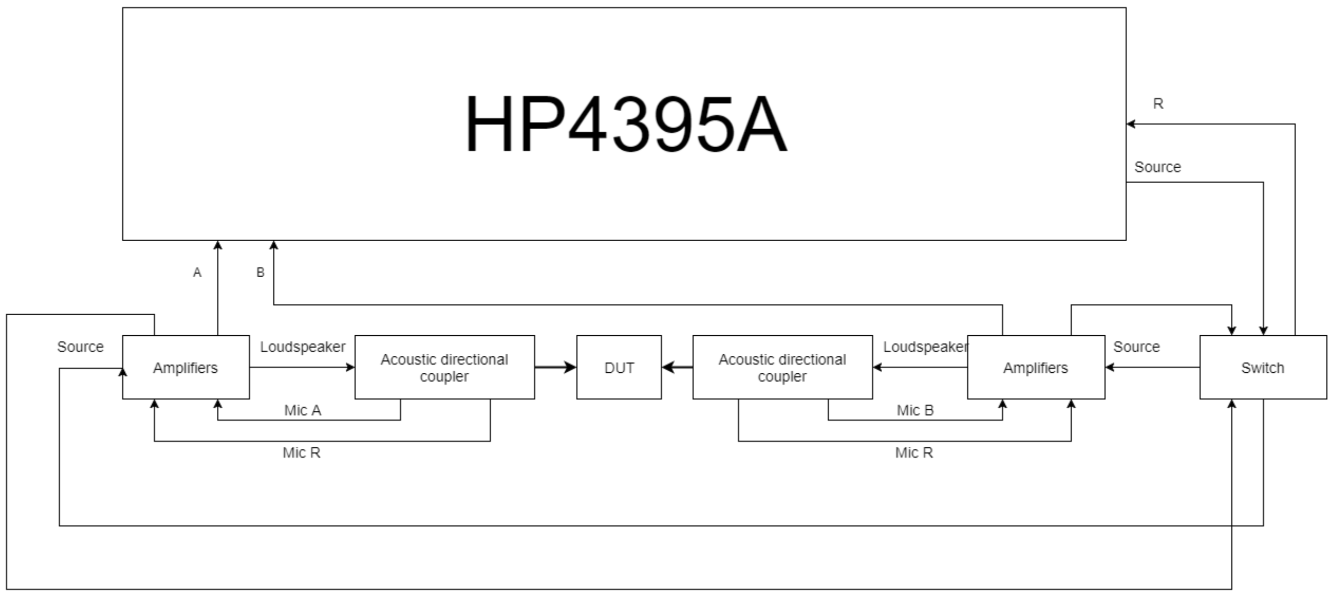

Fig. 3. A block diagram of the hardware required for the acoustic VNA. The R, A and B signals refer to microphone signals, where R is the 'reference' microphone or FWD coupled signal and A and B are the REV coupled signals of either port. So S_{11} is the ratio of A/R and S_{21} is the ratio of B/A. DUT stands for 'Device under test'.

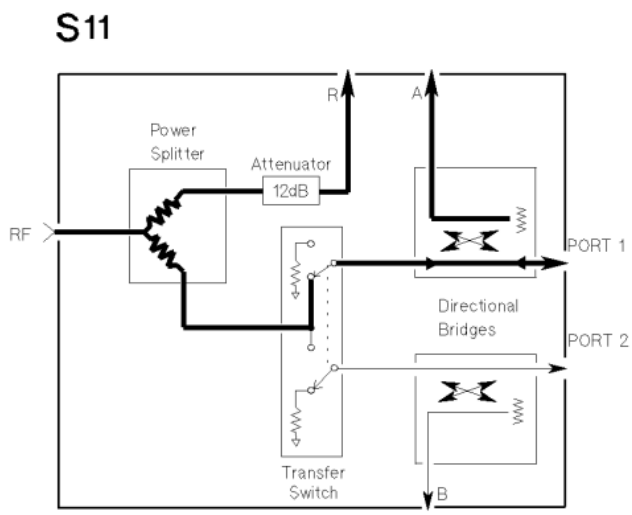

Fig. 4. Block diagram of the 87511A test-set configured to measure S_{11}. [6]

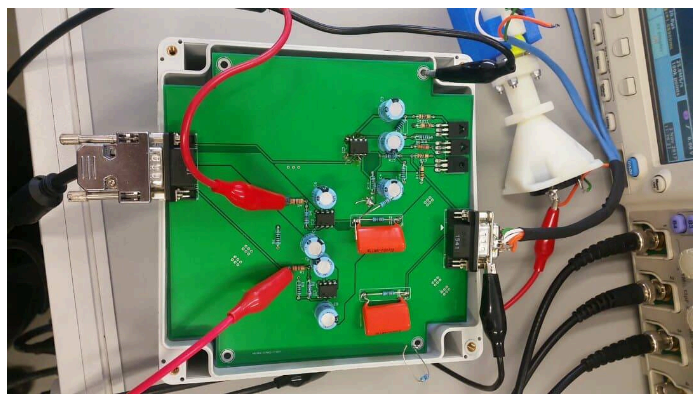

Fig. 5. Remote head PCB assembly.

The Dayton audio ND20FB-4 is a 4 Ω tweeter with a usable frequency range of 3.5–25 kHz, making it suitable for the 10–20 kHz coupler set. Its rear mount design makes it ideal for mounting to the coupler via a horn waveguide.

The microphones used are the MP23AB02B, a high-performance analog bottom-port MEMS (Micro-electromechanical systems) device. The MP23AB02B covers the full audible frequency range but becomes more responsive at frequencies above 15 Hz. Its characteristics above 20 kHz are not specified.

The frequency response of the speaker and microphones will have some effect on the overall response of the system but these can ultimately be corrected via calibration.

In figure 8 the MEMS microphone can be seen mounted to a PCB that is turn mounted to the coupler, the assembled flange for the horn-coupler interface can also be seen.

C. Acoustic Gotchas

In a conventional network analyser, the generator and receiver are phase locked and sweep simultaneously through the desired frequency span. The speed of acoustic signals ($\approx$ 340 ms^{-1}) is much slower than the speed of light ($\approx$ $300 * 10^6$ ms^{-1}), therefore in the acoustic domain the signal being measured would not be the same frequency as the signal at the source. This is due to the energy taking milliseconds

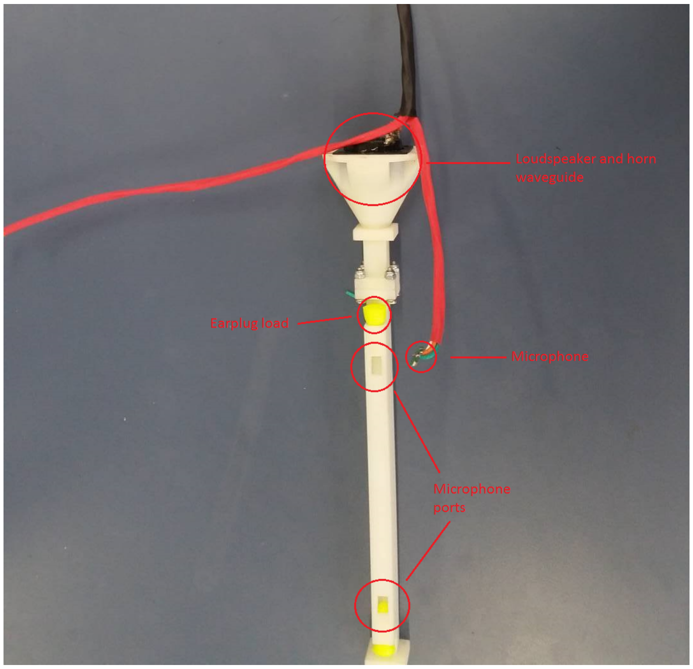

Fig. 6. Coupler assembly for the remote head.

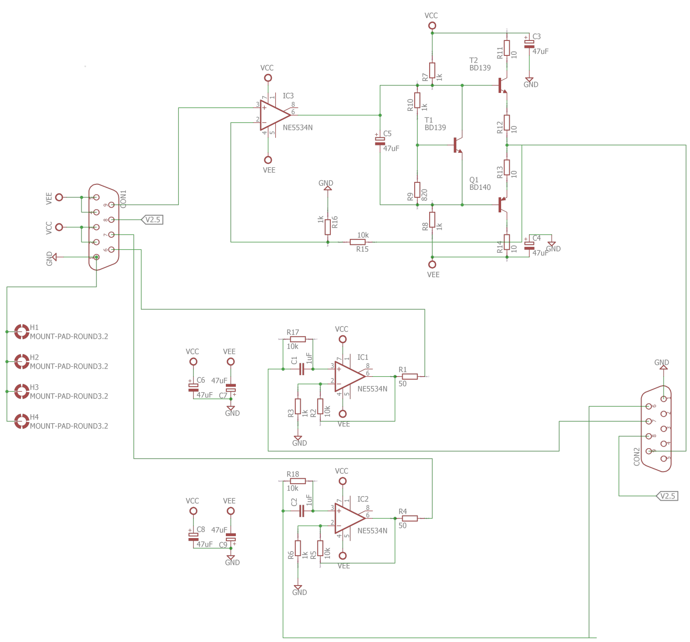

Fig. 7. Remote Head PCB Schematic, contains three audio amplifiers designed to interface the HP3495A with the acoustic waveguide.

to propagate through the hardware. Without allowing for this huge difference in propagation speed, results will make very little sense. The dwell time specifies the time the generator stays at each frequency step in the sweep before the analyser takes the measurement. The sweep speed must be considerably reduced so that the energy has time to bounce back and forth a few times through the test setup before data is captured.

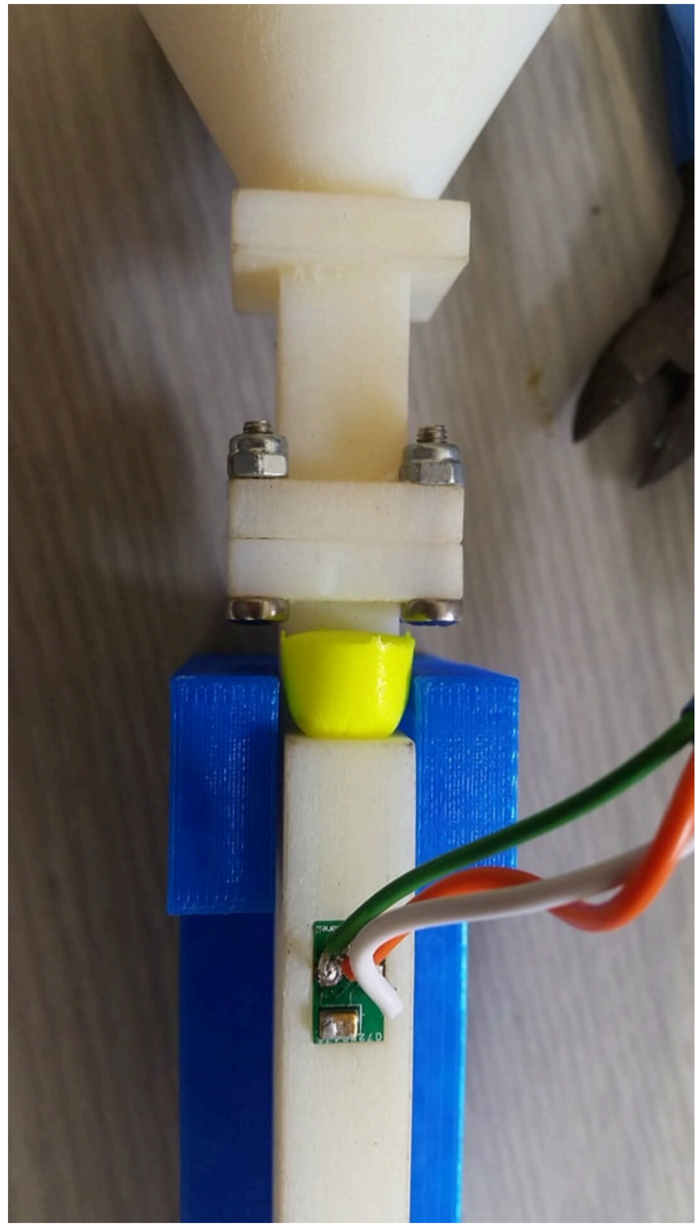

Fig. 8. Coupler assembly with mounted microphones and loudspeaker.

Next, the phase delay through the setup is relatively huge. This means that a small change in frequency causes a huge change in phase. Any practical number of points in a sweep give random-looking results on a Smith chart. Port extension compensates for the phase shift of an extended measurement reference plane due to cables, adapters, and fixtures. Port extension is used predominantly when a calibration is unable to be performed directly at the device or at a convenient place. In this case we are as yet unable to calibrate, but we need to compensate for the (electrical) length of waveguide in the system. This is done by estimating the length of time waves will take to propagate within the waveguide system, and adjusting the port extension so as to “unravel” the data points on the display.

III. Results

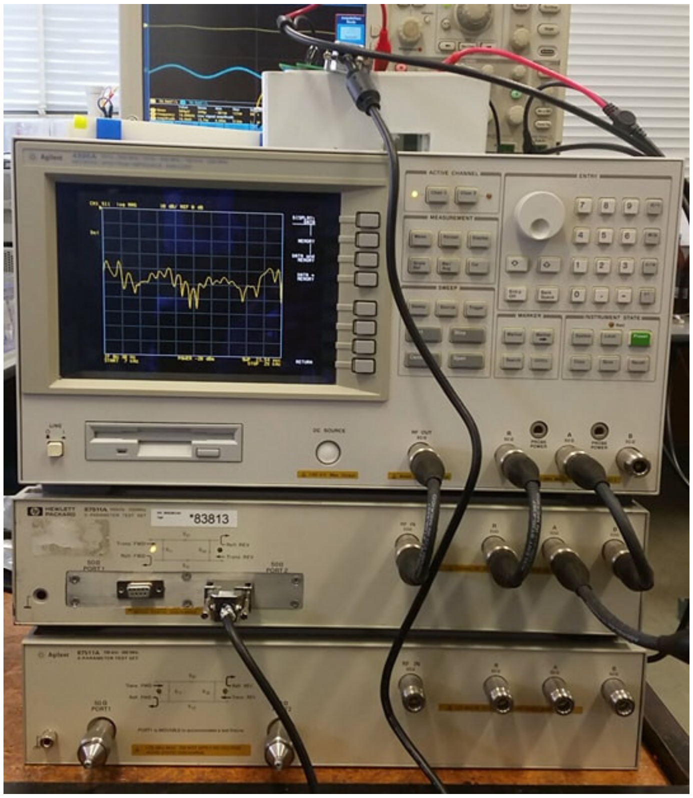

Fig. 9. AVNA set-up.

Figure 9 shows the AVNA set-up. The amplifier PCB is connected to the test-set and coupler assembly via DB9 connectors, the microphones are powered by an internal power supply, as is the amplifier PCB. A Tektronix MSO 4054 oscilloscope was used to check levels, monitor operation, and ensure there was no system failure during measurement. (Setup is still fragile at this stage.)

By using the data-to-memory and math functions, traces can be shown for multiple S_{11} measurements on the instrument display. Figure 10 captures key results for the 10–20 kHz coupler.

The blue trace shows uncalibrated S_{11} with the port terminated with a titanium plate that is assumed to be very reflective with negligible transmission. The assumption that the titaniums is very reflective is made because of the thickness and stiffness of the titanium plate. The plate was laser sintered and can be seen in figure 11.

The yellow trace has the port terminated with a load in the form of an ear plug. With appropriate dwell time and port extension the Smith chart has been made to display sensible uncalibrated results.

In this case the coupler is nearly 200 mm in total length so a port extension was made to approximately 200–300 μs, corresponding to approximately 70–100 mm. For our larger couplers the port extensions will need to be in the order of milliseconds.

Fig. 10. Both S_{11} traces for the metal reflect and the load as displayed on the HP4395A screen. The smith chart shows amplitude information as a ratio of the source power (therefore always ≤ 1) as the distance from the center, position indicates phase, the arcs from the outside of the circle to the far right are lines of constant phase.

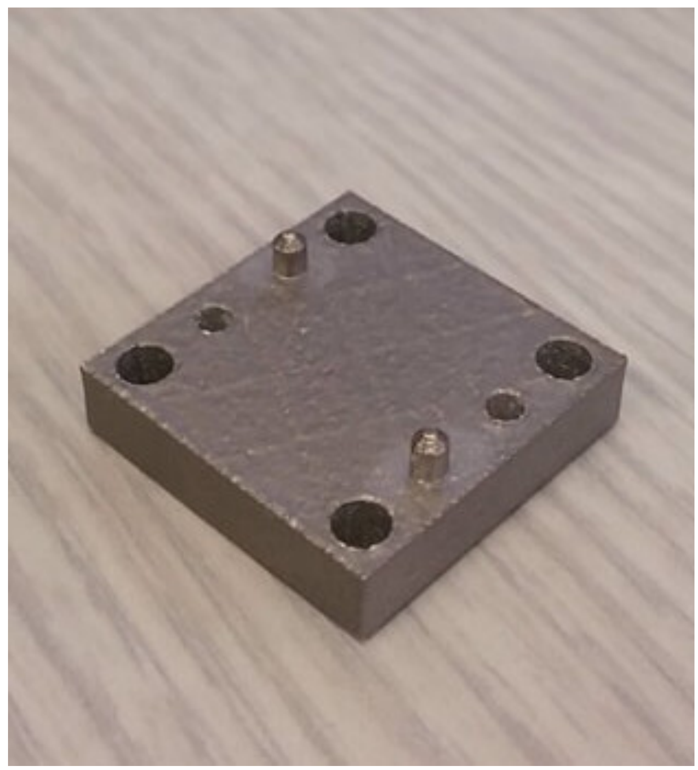

Fig. 11. The laser sintered (3D printed) titanium 'reflect' standard. It's unclear what effect if any the surface finish may have on the 'reflect' standard.

These S_{11} measurements on the Smith chart show the trace collapses closer to the center of the chart when a load is placed on the port, and conversely expands with a reflect, consistent with theory.

The loops in the traces indicate that there may be some resonances in the system. These can be accounted for in the

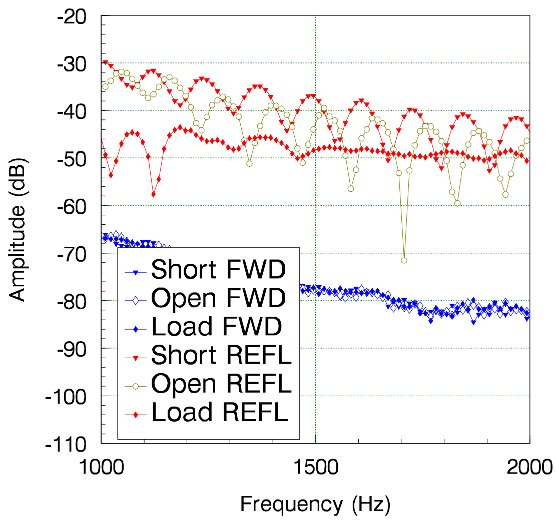

Fig. 12. Measurements for a Short, Open and Load with the 1–2 kHz coupler system.

future with calibration. The port extension function can also effect the number of loops in the trace. It is common to see these loops 'unravel' with more extension and then reappear as the extension goes too far, this can be used to tune the port extension where minimising the number of loops optimise's the extension. These loops are related to the phase of the wave which can be be impacted by the combination of dwell time, port extension, standing waves in the waveguide and vibration of the waveguide itself transmitting energy. Vibration of the waveguide could introduce difficulties in performing two port measurements which can be compensated for with calibration.

Figure 12 shows similar data captured using the 1–2 kHz coupler, this log-mag plot (no phase information) shows similar results to the 10–20 kHz coupler for a reflect and load. This plot shows the individual signals seen by the HP4395A for the 'R' and 'A' signals, as expected the forward coupled signal 'R' changes very little in each case and the 'A' signal changes in each case, with measured magnitude increasing generally with the reflect and decreasing generally with a load.

IV. Conclusion

These S_{11} measurements show that the system works as expected. The load and reflect measurements show that the hardware is functional by demonstrating directionality and producing data that aligns with expectations of acoustically absorbent and reflective materials. These measurements also attest to the ability of the waveguide hardware to be interfaced with the HP4395A.

Some aspects of the calibration are going to be challenging in achieving a dual port system. All calibration code will have to be developed, and it will need to include the oft-omitted isolation terms, irrelevant in many EM scenarios, but suspected to be inescapable in the acoustic situation, as sound travels through all matter. [8] [9]

References

[1] ASTM Standard C384, 2004, "Standard test method for impedance and absorption of acoustical materials by impedance tube method".

[2] Doug Rytting ARFTG 50 Year Network Analyser History Rytting Consulting, Santa Rosa, California, 95405, USA

[3] M. MacDonell, 'Scaling acoustic directional couplers using 3D printing', Thesis, Master of Engineering (ME), University of Waikato, 2015.

[4] Scott, J. and K. E. Pennington, "Acoustic Vector-Corrected Impedance Meter", *IEEE Transactions on Instrumentation and Measurement, 2014. DOI: 10.1109/TIM.2014.2327474*

[5] Lagasse, P., "Realisation of an acoustical directional coupler", Journal of sound and vibration*, 15(3), April 1971, pp367–372.*

[6] HP87511A User manual.

[7] HP4395A User Manual

[8] Network Analyser Error Models and Calibration Methods by Doug Rytting

[9] Agilent AN 1287-3 Applying Error Correction to Network Analyser Measurements

[10] ISO 10534-1:1996 Acoustics – Determination of sound absorption coefficient and impedance in impedance tubes – Part 1: Method using standing wave ratio

[11] ISO 10534-2:1998 - Acoustics – Determination of sound absorption coefficient and impedance in impedance tubes – Part 2: Transfer-function method

[12] http://www.keysight.com/en/pdx-x202277-pn-N5242A/pna-x-microwave-network-analyzer-265-ghz?cc=NZ&lc=eng

[13] https://www.nsi-mi.com/products/system-solutions/near-field-systems

[14] http://www.mwrf.com/sites/mwrf.com/files/styles/article_featured_standard/public/uploads/2012/12/25aoml_0.jpg?itok=DeRbx8FU